

Structural and Spectroscopic Characterization of a Monomeric Side-On Manganese(IV) Peroxo Complex**

Chien-Ming Lee,* Chi-He Chuo, Ching-Hui Chen, Cho-Chun Hu, Ming-Hsi Chiang,* Yu-Jan Tseng, Ching-Han Hu, and Gene-Hsiang Lee

Manganese ions are present in the active sites of several enzymes that are involved in important reactions, such as activation of molecular oxygen, detoxification of superoxide and hydrogen peroxide, and water-splitting chemistry.^[1] In the catalytic cycles of these enzymes, Mn-superoxo or Mn-peroxo complexes have been implicated as reactive intermediates. For example, a Mn^{III}-superoxo or Mn-peroxo-HPCA radical adduct is proposed in Mn-dependent homoprotocatechuate (HPCA) 2,3-dioxygenase, which catalyzes the ring opening of HPCA with incorporation of both oxygen atoms from O₂.^[2] In synthetic systems, most of the peroxomanganese complexes like the Co,^[3] Ni,^[4] Cu,^[5] and Fe^[6] analogs are generated from the H₂O₂ source. Few examples for the Mn^{II}-mediated reduction of O₂ yielding the Mn–O₂ adduct were reported.^[7–10] Hoffman and co-workers reported that Mn^{II}TPP(py) can act as an oxygen carrier at low temperature to form a Mn–(TPP)(O₂) complex with a Mn^{IV}(O₂)^{2–} formalism and the binding mode of the peroxo ligand was suggested as symmetric side-on.^[7] Another example reported by the Wiegardt group is the binuclear [L₂Mn₂(μ-O)₂(μ-O₂)]²⁺ complex, which contains a peroxo bridge between two Mn^{IV} ions.^[9] Recently, Borovik and co-workers showed that reaction of [Mn^{II}H₂bupa][–] and O₂ at ambient temperature produces monomeric Mn^{III}-peroxo complexes.^[10] In this system, the noncovalent interactions (hydrogen bonding) within the secondary coordination sphere support the activation of O₂.^[11] In this report, we demonstrate that the complex [Mn^I(CO)₃(P(C₆H₃-3-SiMe₃-2-S)₂(C₆H₃-3-SiMe₃-2-SH))][–], **1b**, with the pendant thiol group in the secondary coordina-

tion sphere can activate molecular oxygen, leading to the formation of the monomeric, O₂-side-on-bound Mn^{IV} complex, [Mn(O₂)(P(C₆H₃-3-SiMe₃-2-S)₂)][–], **3**.

Reaction of *cis*-[Mn(CO)₄(SC₆H₅)₂][–] with one equivalent of P(C₆H₃-3-R-2-SH)₃ (R = H or SiMe₃) in tetrahydrofuran (THF) solution at 50 °C, respectively, produced the six-coordinate [Mn(CO)₃(P(C₆H₃-3-R-2-S)₂(C₆H₃-3-R-2-SH))][–] (R = H, **1a**; SiMe₃, **1b**) isolated as a yellow solid in high yield (95 % for **1a**; 92 % for **1b**). The IR spectra of **1a** and **1b** show the same CO stretching bands at 1989(vs), 1908(s), and 1886(s) (Figure 1), consistent with a tricarbonyl derivative possessing pseudo C_{3v} symmetry.^[12] Complex **1a** can be crystallized by vapor diffusion of diethyl ether into a concentrated THF/CH₃CN (3:1, v/v) solution at –20 °C in nitrogen.^[13] Figure 1 displays a thermal ellipsoid plot of **1a**. The manganese center is coordinated by one phosphorus, two thiolate sulfur atoms, and three CO groups in a facial position, in agreement with the infrared data. The structural data also reveal that **1a** contains a pendant thiol group in the secondary coordination sphere. An intramolecular [C≡O⋯H–S] interaction (the S(3)⋯O(3) distance of 3.526 Å found in **1a**) is present, which is responsible for the broadening of the S–H stretching band. The stretching vibrations ν_{S–H} (in the range of 2500–2000 cm^{–1}) of complexes **1a** and **1b** were not identified.^[14] Similarly, attempts to identify the chemical shifts of the thiol protons in **1a** and **1b** by NMR spectroscopy were not successful.

Addition of an excess of molecular oxygen to a THF solution of **1a** at ambient temperature for 1 h affords an orange-red complex **2**. The electrospray ionization mass (ESI-MS) spectrum of the oxygenated species shows a maximum ion peak at 409.8 (a mass-to-charge ratio, Figure S1 in the

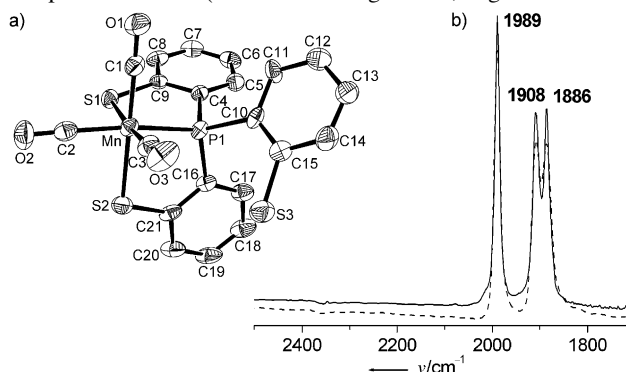


Figure 1. a) ORTEP diagram of [Mn(CO)₃(P(C₆H₄-2-S)₂(C₆H₄-2-SH))][–], **1a**, with thermal ellipsoids at 50% probability and hydrogen atoms omitted for clarity, and b) FTIR spectra of **1a** (solid) and **1b** (dash) measured in the absorbance mode. Selected bond distances [Å]: Mn–S1 2.3919(11), Mn–S2 2.3929(12), Mn–P1 2.2584(11).

[*] Prof. C.-M. Lee, C.-H. Chuo, C.-H. Chen, Prof. C.-C. Hu
Department of Applied Science, National Taitung University
Taitung city 950 (Taiwan)
E-mail: cmlee@nttu.edu.tw

Dr. M.-H. Chiang
Institute of Chemistry, Academia Sinica
Nankang, Taipei 115 (Taiwan)
E-mail: mhchiang@chem.sinica.edu.tw

Y.-J. Tseng, Prof. C.-H. Hu
Department of Chemistry
National Changhua University of Education
Changhua 500 (Taiwan)

Dr. G.-H. Lee
Instrumentation Center, National Taiwan University
Taipei 107 (Taiwan)

[**] We thank the National Science Council (Taiwan) for financial support (NSC 99-2113-M-143-002-MY2), and Prof. Wen-Feng Liaw and Dr. Feng-Chun Lo for helpful discussions.

Supporting information for this article is available on the WWW under <http://dx.doi.org/10.1002/anie.201201735>.

Supporting Information), which is the signature of $[\text{Mn}^{\text{II}}(\text{P}(\text{C}_6\text{H}_4\text{-}2\text{-S})_3)_2]^{2-}$ (calcd m/z 409.9). The crystallographic analysis of single crystals of **2** supports this assignment (Figure 2). Prolonged stirring of the mixture generates insoluble yellow solid. Attempts to isolate the insoluble yellow solid were unsuccessful.

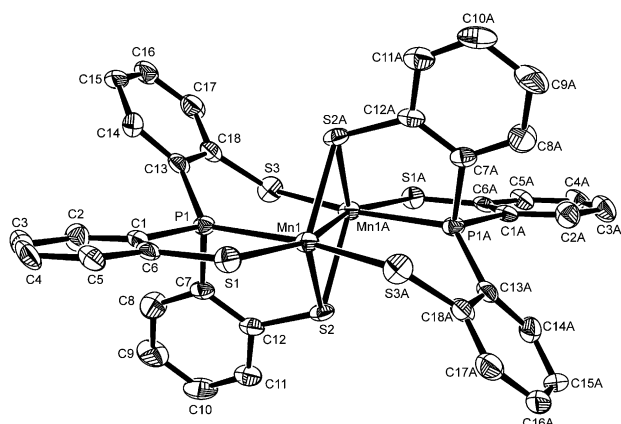


Figure 2. ORTEP diagram of $[\text{Mn}^{\text{II}}(\text{P}(\text{C}_6\text{H}_4\text{-}2\text{-S})_3)_2]^{2-}$, **2**, with thermal ellipsoids at 50% probability and hydrogen atoms omitted for clarity. Selected bond distances [Å]: Mn1–S1 2.412(2), Mn1–S2 2.491(2), Mn1–S2A 2.517(2), Mn1–S3A 2.453(3), Mn1–P1 2.687(2), and Mn1–Mn1A 2.969(2).

In contrast, treating **1b** with excess molecular oxygen in THF solution at room temperature for 1 h generates the monomeric O_2 -side-on-bound $[\text{Mn}(\text{O}_2)(\text{P}(\text{C}_6\text{H}_3\text{-}3\text{-SiMe}_3\text{-}2\text{-S})_3)]^-$, **3**. When reaction of **1b** and excess O_2 in THF was monitored by UV/Vis spectroscopy at ambient temperature (Figure S2 in the Supporting Information), three features at 490, 550, and 755 nm gradually developed with decrease of a band at 395 nm, indicating the formation of **3**. Two absorption bands (at 490 and 550 nm) in the visible region may be attributed to d–d transitions for the d^3 ions.^[15] The infrared spectrum (KBr) of **3** measured at room temperature shows a feature at 903 cm^{-1} , which is consistent with the O–O stretching frequency for a peroxometallic complex ($\nu_{\text{O-O}} \approx 800\text{--}930\text{ cm}^{-1}$).^[16] When $^{18}\text{O}_2$ was used instead, the corresponding $^{18}\text{O}\text{--}^{18}\text{O}$ vibration was not observed because of overlap with intense $\nu_{\text{Si-C}}$ bands found between 845 and 875 cm^{-1} (Figure 3). The difference spectrum of **3** and its ^{18}O -labeled derivative shows that the $\nu_{\text{O-O}}$ band of ^{18}O -labeled **3** shifts to around 861 cm^{-1} (inset in Figure 3), roughly similar to the calculated position based on the difference in masses of the ^{16}O - and ^{18}O -labeled compounds. The $^{16}\text{O}\text{--}^{16}\text{O}$ vibration of complex **3** is slightly higher than those (around $885\text{--}896\text{ cm}^{-1}$) reported for the monomeric η^2 -peroxo Mn^{III} systems^[11,17] and the thiolate-ligated manganese(III)-alkylperoxo species.^[18] On the other hand this vibration is red-shifted by 80 cm^{-1} compared to the $\text{Mn}(\text{TPP})(\text{O}_2)$ complex.^[8] The results from reactions carried out in an $^{18}\text{O}_2$ atmosphere also indicate that O_2 is the source for the formation of **3**. The ESI-MS spectra of the oxygenated species of **1b** shows a maximum ion peak at 658.1 m/z (Figure S3 in the Supporting Information), consistent with the mass and calculated isotope distribution of the $[\text{Mn}(\text{O}_2)(\text{P}(\text{C}_6\text{H}_3\text{-}3\text{-SiMe}_3\text{-}2\text{-S})_3)]^-$ anion (calcd, 658.0 m/z). Furthermore, the shift of four mass units to a m/z value of

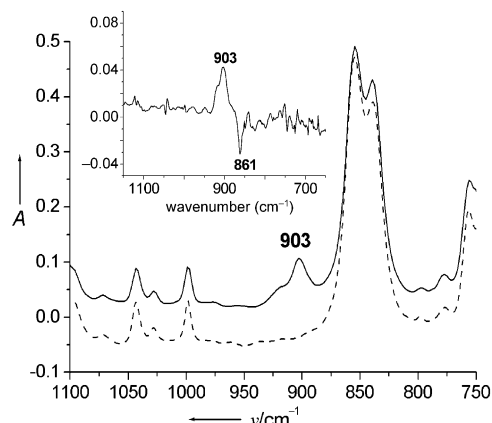


Figure 3. FTIR spectra of **3** (solid line) and ^{18}O -labeled **3** (dashed line). Inset: a difference spectrum between **3** and its ^{18}O -labeled derivative.

662.1 (calcd, 662.0 m/z) when $^{18}\text{O}_2$ was used in the reaction (Figure S4 in the Supporting Information) supports the assignment to $[\text{Mn}(\text{O}_2)]^-$.

The molecular structure of **3** is given in Figure 4. Complex **3** contains a side-on 1:1 Mn– O_2 moiety with the tetradentate ligand $[\text{P}(\text{C}_6\text{H}_3\text{-}3\text{-SiMe}_3\text{-}2\text{-S})_3]^{3-}$. The dioxygen is almost symmetrically bound to the Mn ion with the mean Mn–O distance of $1.878(2)\text{ Å}$, which is longer than the average $\text{Mn}^{\text{IV}}\text{--O}_{\text{peroxo}}$ distance of $1.83(2)\text{ Å}$ in binuclear $[\text{L}_2\text{Mn}_2(\mu\text{-O})_2(\mu\text{-O}_2)]^{2+}$ complexes.^[9] The mean Mn–O distance of **3** falls into the range of $1.841\text{--}1.901\text{ Å}$ for the monomeric side-on peroxomanganese(III) complexes.^[17,19,20] An acute angle of $43.07(11)^\circ$ of $\angle \text{O}_{\text{peroxo}}(1)\text{--Mn--O}_{\text{peroxo}}(2)$ causes a highly distorted octahedral coordination geometry around the manganese site. The Mn ion shows a large deviation of $0.4472(6)\text{ Å}$ from the least-square plane based on the three phenylthiolate sulfur atoms. The O–O bond length

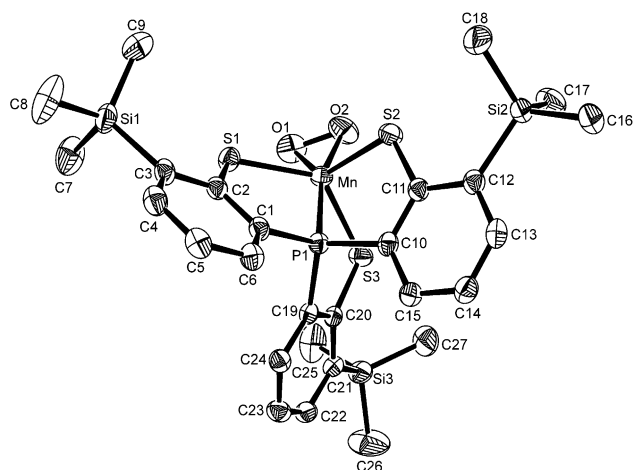


Figure 4. ORTEP drawing of $[\text{Mn}(\text{O}_2)(\text{P}(\text{C}_6\text{H}_3\text{-}3\text{-SiMe}_3\text{-}2\text{-S})_3)]^-$, **3**, with thermal ellipsoids at 50% probability and hydrogen atoms omitted for clarity. Selected bond distances [Å] and angles [deg]: O1–O2 1.379(3), Mn–S1 2.3370(8), Mn–S2 2.3836(8), Mn–S3 2.3857(8), Mn–P1 2.3036(8), Mn–O1 1.883(2), Mn–O2 1.873(2), O1–Mn–O2 43.07(11), S1–Mn–S2 110.25(3), S1–Mn–S3 130.59(3), S2–Mn–S3 108.34(3), S1–Mn–P1 80.92(3), S2–Mn–P1 79.89(3), S3–Mn–P1 76.69(3), P1–Mn–O1 149.60(8), P1–Mn–O2 164.46(9).

of 1.379(3) Å in **3** is slightly shorter than those bond lengths of the structurally characterized monomeric η^2 -peroxomanganese(III) complexes (1.40–1.43 Å).^[17,19,20] The transfer of less charge from the high-valent Mn^{IV} ion to the coordinated peroxy ligand relative to the charge transfer in monomeric side-on peroxomanganese(III) complexes may account for the shorter O–O bond length and the higher $\nu_{\text{O-O}}$ of **3**.^[21]

Analyses of structural data (O–O bond length) and vibrational energy ($\nu_{\text{O-O}}$) reveal that the dioxygen ligand of **3** could be described as a peroxy type that is further confirmed by EPR, SQUID as well as DFT computation. The X-band EPR spectrum of **3** recorded at 4 K deviates from the ideal axial pattern with two broad signals (Figure 5a). One strong

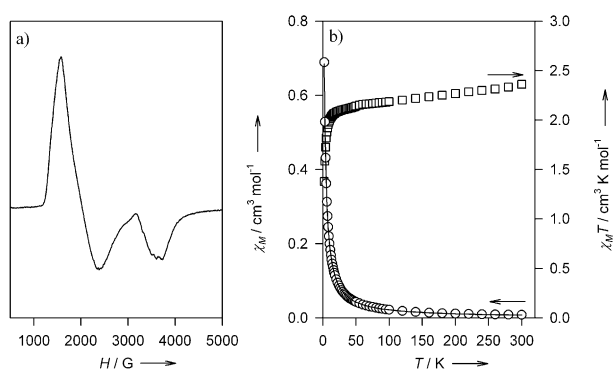


Figure 5. a) X-band EPR spectrum of **3** at 4 K and b) plots of magnetic susceptibility (open circles) and $\chi_M T$ (open squares) versus the temperature for **3**. The solid line is the best fit to the theoretical model.

band at $g = 4.37$ and a weak one at $g = 1.91$ are observed. No ⁵⁵Mn hyperfine coupling can be resolved for both. The observed result is in agreement with the known spectra for the Mn^{IV} species.^[7,15,22] From dominance of the low-field resonance, it is expected that energy between two Kramer's doublets of the $S = 3/2$ manifold is larger than 0.31 cm⁻¹. The value of D is estimated to be around 0.42 cm⁻¹ if g_{\perp}^e is around 3.40 and g_{\perp} and g_{\parallel} are around 1.91.^[23] The magnetic study of **3** suggests that it is a quartet state complex. The $\chi_M T$ value of **3** remains around 2.1 cm³ K mol⁻¹ in a temperature range of 20 to 300 K, consistent with the presence of the high-spin Mn^{IV} center (Figure 5b). The rapid drop of the $\chi_M T$ value below 20 K is probably attributed to a contribution of zero-field splitting (ZFS) and/or intermolecular antiferromagnetic interactions. The best fit ($R^2 = 0.9999$) to the temperature-dependent $\chi_M T$ data reveals $g = 2.14$ and $D = 0.68$ cm⁻¹. The axial ZFS parameter deduced from the magnetic measurement is comparable with that from the EPR study, suggesting the decrease of $\chi_M T$ is primarily due to depopulation of the excited state.

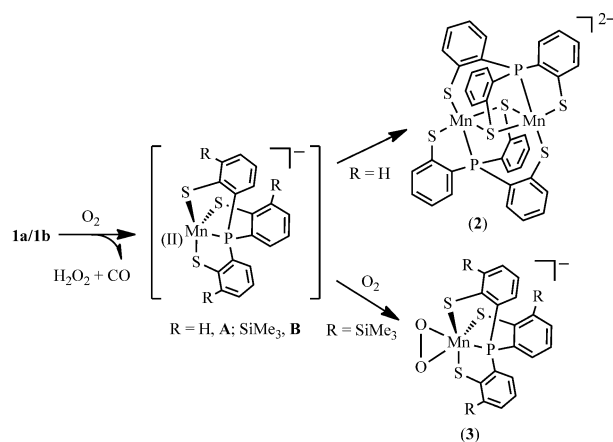
The geometries of the doublet, quartet, and sextet states of **3** were optimized using mPWPW91/6-31G(d). The quartet state was found to be the lowest energy species, while the doublet and sextet state lie 12.3 and 14.6 kcal mol⁻¹ higher in energy (ΔG at 298 K), respectively. The O–O bond distance, ¹⁶O–¹⁶O and ¹⁸O–¹⁸O stretching frequencies, atomic charges

Table 1: O–O distance (Å; $R_{\text{O-O}}$), ¹⁶O–¹⁶O and ¹⁸O–¹⁸O stretching frequencies (cm⁻¹; $\nu_{16\text{O-}16\text{O}}$, $\nu_{18\text{O-}18\text{O}}$), natural population analysis charges of the O₂ moiety and the metal ($q_{\text{O-O}}$ and q_{Mn}), and the Wiberg bond index for O–O and Mn–O bonds (O-O_{WBI} and Mn-O_{WBI}).

	Doublet	Quartet	Sextet
$R_{\text{O-O}}$	1.398	1.427	1.339
$\nu_{16\text{O-}16\text{O}}$	975	959	1130
$\nu_{18\text{O-}18\text{O}}$	921	906	1064
$q_{\text{O-O}}$	-0.7034	-0.7795	-0.5650
q_{Mn}	1.1432	1.3286	1.3425
O-O_{WBI}	1.095	1.071	1.231
Mn-O_{WBI}	0.613/0.783	0.604/0.610	0.172/0.340

out of natural population analysis for the O₂ moiety and the metal, and the Wiberg bond index for O–O and Mn–O bonds are summarized in Table 1. The O–O distance of the quartet is the longest. This feature is revealed in the smallest stretching frequency and Wiberg bond index between the oxygen atoms. In addition, the atomic spin densities of **3** in the quartet state are 2.769 on Mn (see Table S1 in the Supporting Information), indicating that the unpaired electrons are primarily located in the manganese d orbitals.

The reaction sequences given in Scheme 1 probably account for the formation of **2** and **3**. Molecular oxygen may initially oxidize the pendant thiol groups^[14] of **1a/1b** to form the four-coordinate transient species $[\text{Mn}^{\text{II}}(\text{P}(\text{C}_6\text{H}_3\text{-3-R-2-S})_3)]^-$ ($\text{R} = \text{H}$, **A**; SiMe_3 , **B**), accompanied by the release of CO and the formation of hydrogen peroxide.^[24] The second possible pathway that is gone through direct oxidation of the metal site by O₂ followed by coordination of the dangling thiol group could not be ruled out albeit the manganese center is coordinatively saturated in **1a** and **1b**.^[25] The attempt to isolate **A/B** is fruitless. In solution, coexistence of the starting materials and the products except for **A/B** was observed by spectroscopy. We tentatively propose that dimerization proceeds upon formation of **A** to afford **2**. On the other hand, the steric hindrance resulting from the SiMe₃ groups of **B** inhibits dimerization and constitutes a pocket open to the O₂ binding (Figure S5 in the Supporting Information). Treatment of Mn^{II} complexes with superoxides or peroxides in the presence of Lewis bases generates



Scheme 1. A proposed mechanism for the formation of **2** and **3**.

peroxomanganese(III) species.^[11,17,19,20,26] Therefore, one can propose that **B** reacts with the second equivalent of O₂ to afford **3**.^[27]

Contrary to the Fe^{III}- and Mn^{III}-peroxo complexes showing high rate constants on aldehyde deformylation at low temperatures,^[20,28] **3** does not react with cyclohexanecarboxaldehyde (CCA, 100 equiv) under the same conditions. The excitation band at 550 nm reveals unobservable changes at room temperature within 1 h. The decreased ability for nucleophilic attack of the substrates could be the result of an electronic influence: electronic deficiency of the Mn center, which is rationalized by its high oxidation state (+4) and the negative reduction potential of -1.51 V (vs. Fc⁺/Fc; Fc = ferrocene; Figure S6 in the Supporting Information).

In summary, we succeeded in the syntheses and structural characterization of a monomeric side-on [Mn^{IV}(O₂)(P(C₆H₃-3-SiMe₃-2-S)₃)⁻ complex, **3**, obtained from oxygenation of **1b** at ambient temperatures. The successful isolation of **3** may be attributed to the steric effect of the bulky SiMe₃ groups on the phenyl rings, which prohibits the monomeric transient species from formation of polymetallic complexes with bridging thiolate groups.^[29] The pocket created by the “picket fence ligand” [P(C₆H₃-3-SiMe₃-2-S)₃]³⁻ allows O₂ binding with the Mn center to form a stable side-on Mn^{IV}-peroxo complex.^[30] Importantly, the binding mode of the peroxo fragment in **3** can support other peroxomanganese(IV) complexes, which are described as key intermediates for the O₂ carrier, or the reversible cleavage/formation of the O–O bond.^[7,22] Further activity studies of **3** are under way.

Received: March 3, 2012

Published online: ■ ■ ■ ■, ■ ■ ■ ■ ■ ■

Keywords: bioinorganic chemistry · coordination modes · enzyme models · manganese · oxygen activation

- [1] a) M. W. Vetting, L. P. Wackett, L. Que, Jr., J. D. Lipscomb, D. H. Ohlendorf, *J. Bacteriol.* **2004**, *186*, 1945–1958; b) A.-F. Miller, *Acc. Chem. Res.* **2008**, *41*, 501–510; c) L. E. Grove, J. Xie, E. Yikilmaz, A.-F. Miller, T. C. Brunold, *Inorg. Chem.* **2008**, *47*, 3978–3992; d) A. J. Wu, J. E. Penner-Hahn, V. L. Pecoraro, *Chem. Rev.* **2004**, *104*, 903–938; e) J. P. McEvoy, G. W. Brudvig, *Chem. Rev.* **2006**, *106*, 4455–4483.
- [2] W. A. Gunderson, A. I. Zatsman, J. P. Emerson, E. R. Farquhar, L. Que, Jr., J. D. Lipscomb, M. P. Hendrich, *J. Am. Chem. Soc.* **2008**, *130*, 14465–14467.
- [3] a) J.-H. Cho, R. Sarangi, H.-Y. Kang, J.-Y. Lee, M. Kubo, T. Ogura, E. I. Solomon, W. Nam, *J. Am. Chem. Soc.* **2010**, *132*, 16977–16986; b) R. Sarangi, J. Cho, W. Nam, E. I. Solomon, *Inorg. Chem.* **2011**, *50*, 614–620.
- [4] J. Cho, R. Sarangi, J. Annaraj, S. Y. Kim, M. Kubo, T. Ogura, E. I. Solomon, W. Nam, *Nat. Chem.* **2009**, *1*, 568–572.
- [5] T. Osako, S. Nagatomo, Y. Tachi, T. Kitagawa, S. Itoh, *Angew. Chem.* **2002**, *114*, 4501–4504; *Angew. Chem. Int. Ed.* **2002**, *41*, 4325–4328.
- [6] J. Cho, S. Jeon, S. A. Wilson, L. V. Liu, E. A. Kang, J. J. Braymer, M. H. Lim, B. Hedman, K. O. Hodgson, J. S. Valentine, E. I. Solomon, W. Nam, *Nature* **2011**, *478*, 502–505.
- [7] a) C. J. Weschler, B. M. Hoffman, F. Basolo, *J. Am. Chem. Soc.* **1975**, *97*, 5278–5280; b) B. M. Hoffman, C. J. Weschler, F. Basolo, *J. Am. Chem. Soc.* **1976**, *98*, 5473–5482.
- [8] M. W. Urban, K. Nakamoto, F. Basolo, *Inorg. Chem.* **1982**, *21*, 3406–3408.
- [9] U. Bossek, T. Weyhermueller, K. Wieghardt, B. Nuber, J. Weiss, *J. Am. Chem. Soc.* **1990**, *112*, 6387–6388.
- [10] a) R. L. Shook, W. A. Gunderson, J. Greaves, J. W. Ziller, M. P. Hendrich, A. S. Borovik, *J. Am. Chem. Soc.* **2008**, *130*, 8888–8889; b) R. L. Shook, S. M. Peterson, J. Greaves, C. Moore, A. L. Rheingold, A. S. Borovik, *J. Am. Chem. Soc.* **2011**, *133*, 5810–5817.
- [11] R. L. Shook, A. S. Borovik, *Inorg. Chem.* **2010**, *49*, 3646–3660.
- [12] a) W.-F. Liaw, C.-M. Lee, G.-H. Lee, S.-M. Peng, *Inorg. Chem.* **1998**, *37*, 6396–6398; b) C.-M. Lee, G.-Y. Lin, C.-H. Hsieh, C.-H. Hu, G.-H. Lee, S.-M. Peng, W.-F. Liaw, *J. Chem. Soc. Dalton Trans.* **1999**, 2393–2398.
- [13] Many attempts to crystallize **1b** were unsuccessful.
- [14] C.-M. Lee, C.-H. Chen, S.-C. Ke, G.-H. Lee, W.-F. Liaw, *J. Am. Chem. Soc.* **2004**, *126*, 8406–8412.
- [15] D. P. Kessissoglou, X. Li, W. M. Butler, V. L. Pecoraro, *Inorg. Chem.* **1987**, *26*, 2487–2492.
- [16] a) L. Vaska, *Acc. Chem. Res.* **1976**, *9*, 175–183; b) J. S. Valentine, *Chem. Rev.* **1973**, *73*, 235–245.
- [17] a) N. Kitajima, H. Komatsuzaki, S. Hikichi, M. Osawa, Y. Morooka, *J. Am. Chem. Soc.* **1994**, *116*, 11596–11597; b) U. P. Singh, A. K. Sharma, S. Hikichi, H. Komatsuzaki, Y. Morooka, M. Akita, *Inorg. Chim. Acta* **2006**, *359*, 4407–4411.
- [18] M. K. Coggins, J. A. Kovacs, *J. Am. Chem. Soc.* **2011**, *133*, 12470–12473.
- [19] a) R. B. VanAtta, C. E. Strouse, L. K. Hanson, J. S. Valentine, *J. Am. Chem. Soc.* **1987**, *109*, 1425–1434; b) J. Annaraj, J. Cho, Y.-M. Lee, S. Y. Kim, R. Latifi, S. P. de Visser, W. Nam, *Angew. Chem.* **2009**, *121*, 4214–4217; *Angew. Chem. Int. Ed.* **2009**, *48*, 4150–4153.
- [20] M. S. Seo, J. Y. Kim, J. Annaraj, Y. Kim, Y.-M. Lee, S.-J. Kim, J. Kim, W. Nam, *Angew. Chem.* **2007**, *119*, 381–384; *Angew. Chem. Int. Ed.* **2007**, *46*, 377–380.
- [21] C. J. Cramer, W. B. Tolman, K. H. Theopold, A. L. Rheingold, *Proc. Natl. Acad. Sci. USA* **2003**, *100*, 3635–3640.
- [22] S. H. Kim, H. Park, M. S. Seo, M. Kubo, T. Ogura, J. Klajn, D. T. Gryko, J. S. Valentine, W. Nam, *J. Am. Chem. Soc.* **2010**, *132*, 14030–14032.
- [23] a) D. T. Richens, D. T. Sawyer, *J. Am. Chem. Soc.* **1979**, *101*, 3681–3683; b) L. S. Singer, *J. Chem. Phys.* **1955**, *23*, 379–388.
- [24] The amount of H₂O₂ determined by H₂O₂ test strips was about 3 mg L⁻¹ (yield around 2%). The generated H₂O₂ that further reacts with the pendant thiol group of **1b** may be the reason for the low amount of H₂O₂ detected.
- [25] a) E. Nam, P. E. Alokolaro, R. D. Swartz, M. C. Gleaves, J. Pikul, J. A. Kovacs, *Inorg. Chem.* **2011**, *50*, 1592–1602; b) J. A. Kovacs, L. M. Brines, *Acc. Chem. Res.* **2007**, *40*, 501–509.
- [26] a) S. Groni, G. Blain, R. Guillot, C. Policar, E. Anxolabéhère-Mallart, *Inorg. Chem.* **2007**, *46*, 1951–1953; b) S. Groni, P. Dorlet, G. Blain, S. Bourcier, R. Guillot, E. Anxolabéhère-Mallart, *Inorg. Chem.* **2008**, *47*, 3166–3172; c) R. A. Geiger, S. Chattopadhyay, V. W. Day, T. A. Jackson, *J. Am. Chem. Soc.* **2010**, *132*, 2821–2831; d) R. A. Geiger, S. Chattopadhyay, V. W. Day, T. A. Jackson, *Dalton Trans.* **2011**, *40*, 1707–1715.
- [27] a) N. W. Aboeella, E. A. Lewis, A. M. Reynolds, W. W. Brennessel, C. J. Cramer, W. B. Tolman, *J. Am. Chem. Soc.* **2002**, *124*, 10660–10661; b) A. M. Reynolds, B. F. Gherman, C. J. Cramer, W. B. Tolman, *Inorg. Chem.* **2005**, *44*, 6989–6997.
- [28] J. Annaraj, Y. Suh, M. S. Seo, S. O. Kim, W. Nam, *Chem. Commun.* **2005**, 4529–4531.
- [29] C. A. Grapperhaus, M. Y. Darensbourg, *Acc. Chem. Res.* **1998**, *31*, 451–459.
- [30] J. P. Collman, R. R. Gagne, C. Reed, T. R. Halbert, G. Lang, W. T. Robinson, *J. Am. Chem. Soc.* **1975**, *97*, 1427–1439.

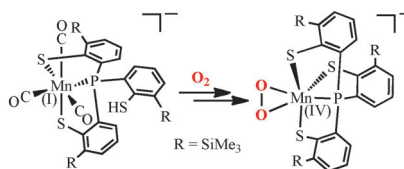
Communications



Oxygen Activation

C.-M. Lee,* C.-H. Chuo, C.-H. Chen,
C.-C. Hu, M.-H. Chiang,* Y.-J. Tseng,
C.-H. Hu, G.-H. Lee ——— ■■■■-■■■■

Structural and Spectroscopic
Characterization of a Monomeric Side-On
Manganese(IV) Peroxo Complex



Gotcha: The binding and activation of oxygen by a manganese complex is reported. A PS_3 coordination sphere built around a manganese(I) center facilitates the isolation of a monomeric manganese(IV) peroxo complex that is stable at ambient temperature (see picture). The activation of molecular oxygen is proposed via a manganese(II) intermediate with an empty site for the binding of the substrate.